

Heating and small-size instantons in the $O(3)$ σ model on the lattice

Federico Farchioni and Alessandro Papa

Dipartimento di Fisica dell'Università and I.N.F.N.

Piazza Torricelli 2, I-56126 Pisa, Italy.

We study the role of small-size instantons in the determination of the topological susceptibility of the 2-d $O(3)$ σ model on the lattice. In particular, we analyze how they affect the non-perturbative determination, by Monte Carlo techniques, of the renormalizations on the lattice. As a result, we obtain a high-precision non-perturbative determination of the mixing with the unity operator, finding good agreement with perturbative computations. We also obtain the size distribution of instantons in the physical vacuum up to very small values of the size in physical units, without observing any ultraviolet cut-off. Moreover, we show by analytical calculation that the mixing of the topological susceptibility with the action density is a negligible part of the whole non-perturbative signal.

I. INTRODUCTION

Simulating a theory on the lattice is the only reliable instrument to study its non-perturbative aspects: the lattice theory, merely being an UV regularized version of the theory on the continuum, takes into account all non-perturbative fluctuations. Some quantities of physical interest, which can be extracted from the lattice, are related to vacuum expectation values of composite operators. Lattice Monte Carlo simulations give a numerical estimate of the cut-off-dependent *bare* expectation values, while the physical quantities on the continuum are the *renormalized* expectation values, which are cut-off-independent. So, the physical quantities can be determined from the lattice only if the renormalizations of the lattice-regularized operators are completely under control.

Perturbation theory has been, up to now, the only mean for the evaluation of the lattice renormalization constants. In particular, perturbative techniques, combined with Monte Carlo simulations, have been applied to the problem of the determination from the lattice of the topological susceptibility of the *QCD* vacuum [1] [2]. The situation has recently changed, since a new method for the determination of the renormalizations of the lattice topological susceptibility has been found [3] [4]. This method, known in literature as the “heating” method, is fully non-perturbative since it relies only on Monte Carlo techniques. Applications to CP^{N-1} models [5] and $SU(2)$ Yang-Mills theory [6] have shown a clear agreement with perturbative calculations [6] [7]. In $SU(2)$ it has been possible to obtain also an indirect determination of the gluon condensate, finding agreement with previous standard Monte Carlo determinations [8].

The $O(3)$ σ model is the simplest model displaying a non-trivial topology, and so it appears as the best laboratory to test the heating method. The drawback is that this topology is suspected to be pathological: the semiclassical approximation [10] shows a small-size divergence in the instantons contribution to the partition function. Such an ultraviolet dominated topology is expected to strongly affect the heating method, which relies on a decoupling between short-range perturbative modes and topological fluctuations, assumed to be long ranged.

In fact, the method had its first application just in $O(3)$ σ model [4] [9], but the statistical fluctuations in the numerical results of those first works are likely to mask an eventual exotic behavior of the model; so, a more accurate investigation on the matter is asked for.

In the present work we perform a careful analysis of the heating method in the $O(3)\sigma$ model to check if, and to what extent, the ultraviolet feature of the topology spoils the non-perturbative determinations of the renormalizations of the lattice susceptibility.

II. THE MODEL

The 2-d $O(3)$ σ model or CP^1 model is described by the Lagrangian:

$$\mathcal{L} = \frac{\beta}{2} \partial_\mu \phi(x) \cdot \partial_\mu \phi(x) \quad , \quad (1)$$

where $\phi(x)$ is a three component real field satisfying the constraint $\phi \cdot \phi = 1$.

The 2-d $O(3)$ σ model plays an important role in quantum field theory because it resembles in several aspects the 4-d non-Abelian gauge theories: asymptotic freedom, non-perturbative behavior in the infrared region with spontaneous mass generation, non-trivial topological structure.

The topological charge of a spin field $\phi(x)$, Q , is the number of times $\phi(x)$ winds the sphere S^2 . It can be expressed as the integral over the space-time of a local operator, $Q(x)$:

$$Q(x) = \frac{1}{8\pi} \epsilon_{\mu\nu} \epsilon_{ijk} \phi_i(x) \partial_\mu \phi_j(x) \partial_\nu \phi_k(x) \quad ; \quad (2)$$

$Q(x)$ is the divergence of a topological current K_μ [11] [12],

$$Q(x) = \partial_\mu K_\mu(x) \quad . \quad (3)$$

All the classical solutions with non-trivial topology, the k -instantons, have been explicitly found [13]. At a quantum level, the only available prediction comes from the semiclassical approximation, which gives for the size distribution of instantons in the physical vacuum:

$$\frac{dN}{Vd\rho} = e^{-4\pi\beta} \beta^2 \frac{f(\rho M)}{\rho^3}, \quad (4)$$

where M is the cutoff mass; renormalization group theory implies

$$f \propto (\rho M)^{4\pi\beta_0}, \quad (5)$$

where $\beta_0 = \frac{1}{2\pi}$ is the one-loop coefficient of the β function; as a result: $dN/d\rho \propto 1/\rho$.

The generalization for CP^{N-1} is: $dN/d\rho \propto \rho^{N-3}$. For $SU(N)$, Eq. (4) and Eq. (5) become respectively

$$\frac{dN}{Vd\rho} = e^{-8\pi^2/g^2} g^{-8} \frac{f(\rho M)}{\rho^5} \quad (6)$$

and

$$f \propto (\rho M)^{16\pi^2\beta_0}; \quad (7)$$

it follows: $dN/d\rho \propto \rho^{\frac{11}{3}N-5}$. For both CP^{N-1} , with $N \geq 4$, and $SU(N)$, the size distribution is suppressed at small sizes with a power law, while in the $O(3)\sigma$ it diverges. This makes $O(3)\sigma$ model singular, and a behavior radically different from the theory of physical interest, QCD , is expected at small distances.

III. THE FIELD THEORETICAL METHOD

We regularize the theory on the lattice by taking the Symanzik tree-level improved action [14]

$$S^L = -\beta \sum_{x,\mu} \left[\frac{4}{3} \phi(x) \cdot \phi(x+\mu) - \frac{1}{12} \phi(x) \cdot \phi(x+2\mu) \right]. \quad (8)$$

In the field theoretical method, a lattice topological charge density operator is defined as a local operator having the appropriate classical continuum limit [15]; our choice is [9]:

$$Q^L = \frac{1}{32\pi} \epsilon_{\mu\nu} \epsilon_{ijk} \phi_i(x) (\phi_j(x+\mu) - \phi_j(x-\mu)) (\phi_k(x+\nu) - \phi_k(x-\nu)). \quad (9)$$

It has been shown in the framework of perturbation theory [9] that the operator $Q(x)$ defined on the continuum is invariant under the renormalization group.

A finite multiplicative renormalization connects the matrix elements of $Q^L(x)$ with those of $Q(x)$ defined on the continuum. The antisymmetry of $Q^L(x)$ forbids mixings with any other $O(3)$ invariant operator of dimension two or less. So, the connection with the continuum is:

$$Q^L(x) = a^2 Z(\beta) Q(x) + O(a^4) . \quad (10)$$

The topological susceptibility is defined on the continuum as the correlation at zero momentum of two topological charge density operators, $Q(x)$:

$$\chi = \int d^2x \langle 0 | T [Q(x)Q(0)] | 0 \rangle . \quad (11)$$

The prescription defining the product of operators in Eq. (11) is [16]

$$\langle 0 | T [Q(x)Q(0)] | 0 \rangle \equiv \partial_\mu \langle 0 | T [K_\mu(x)Q(0)] | 0 \rangle . \quad (12)$$

This prescription eliminates the contribution of possible contact terms (i.e. terms proportional to the δ function or its derivatives) when $x \rightarrow 0$.

The lattice-regularized version of χ is

$$\chi^L = \left\langle \sum_x Q^L(x)Q^L(0) \right\rangle = \frac{1}{L^2} \left\langle \left(\sum_x Q^L(x) \right)^2 \right\rangle , \quad (13)$$

where L is the lattice size.

A prescription equivalent to Eq. (12) does not exist on the lattice, and therefore the contribution of the contact terms must be isolated and subtracted. These contact terms appear as mixings with the action density $S(x)$ and with the unity operator I , which are the only available operators with equal dimension or lower. In formulae

$$\chi^L(\beta) = a^2 Z(\beta)^2 \chi + a^2 A(\beta) \langle S(x) \rangle + P(\beta) \langle I \rangle + O(a^4) , \quad (14)$$

where a is the lattice spacing. In Eq. (14) the quantity $\langle S(x) \rangle$ is intended to be the non-perturbative part of the expectation value of the action density, i.e. it is a signal of dimension two.

$Z(\beta)$ and $P(\beta)$ have been calculated perturbatively in Ref. [9] up to the order $1/\beta^2$ and $1/\beta^5$, respectively.

A relation similar to Eq. (14) holds in $SU(2)$ with the appropriate powers of a and $\langle S(x) \rangle \rightarrow \langle g^2/(4\pi)^2 F_{\mu\nu}^a F_{\mu\nu}^a(x) \rangle$, the gluon condensate. In $SU(2)$, the mixing with the gluon condensate is an appreciable portion of the whole non-perturbative signal in the scaling region, and can be detected through χ^L [6].

We realize that the situation is radically different in the case of the $O(3)$ σ model. Indeed, calculating the leading perturbative contribution to the mixing coefficient, and using a large N result for $\langle S(x) \rangle$ [17] (see Appendix for the details of the calculation and the discussion), we find that the mixing term is smaller than one thousandth of the total non-perturbative signal in the scaling region observed in Ref. [9]. We therefore argue that the contribution to χ^L coming from the mixing term can be safely neglected.

IV. NUMERICAL RESULTS

A. Heating and cooling

Now we want to give a brief account of the heating method (for Ref., see [3] [4]). This method allows a non-perturbative determination of the lattice renormalization constants, $Z(\beta)$ and $P(\beta)$, which have their origin in the short-range fluctuations ($l \sim a$).

Ensembles of configurations $\{C_t\}$ are constructed on the lattice, each configuration of the ensemble being obtained by performing a sequence of t local Monte Carlo sweeps starting from a discretized classical configuration C_0 - a large instanton or the flat configuration. For small t , the heating process does nothing but “switch on” the small-range fluctuations which are responsible for the renormalizations: when the starting configuration is a large instanton (flat configuration), measuring $Q^L(\chi^L)$ on the ensembles $\{C_t\}$, a plateau at the value of $Z(\beta)$ ($P(\beta)$) is expected after a certain time, not depending on β , corresponding to the time of thermalization of quantum fluctuations.

If the heating is protracted, the (local) algorithm of thermalization generates fluctuations of ever increasing size according to the random walk law $l^2 \propto t$.

In the case of the heating of the flat configuration, when the ranges $l \sim \xi_{eq}$ - the equilibrium correlation length - are reached, the contribution of the mixing with the action density to χ^L is thermalized. This is clearly observed in $SU(2)$, where a plateau at a value of χ^L exceeding $P(\beta)$ (perturbatively calculated) of the amount of the expected mixing, is detected [6]. The display of this plateau is possible in $SU(2)$ since the average number of instantons in the first stage of the heating is nearly zero - instantons exhibit a very severe form of critical slowing down. Otherwise, they would start to give a contribution to the topological non-perturbative part of χ^L before the thermalization of the mixing with the action density is reached, so preventing the observation of the plateau.

It is interesting to investigate if this favourable situation happens also in the case of the $O(3)$ σ model; here, the small-size divergence in the instanton size distribution is likely to cause a radical change of the scenario. Since the mixing term is negligible, a plateau is expected at a value of χ^L corresponding to $P(\beta)$. Previous results [4] [9] seem to be in agreement with this expectation; however, the statistical fluctuations of those determinations prevent to absolutely exclude the eventual onset of instanton contribution during the first phase of the heating.

In order to unmask the topological structure of the configurations in the heated ensemble, we use the “cooling” procedure [18]. It consists in a local minimization of the action with the purpose of destroying the quantum fluctuations, trying to preserve the background topological structure. We use an unconstrained cooling, consisting in the following replacement:

$$\phi(x) \rightarrow \phi'(x) = \alpha \sum_{\pm\mu} \left[\frac{4}{3}\phi(x + \mu) - \frac{1}{12}\phi(x + 2\mu) \right] , \quad (15)$$

where α ensures the normalization of the new spin; this replacement exactly minimizes the action when the other spins are kept fixed. We measure the topological charge after each step of cooling. Typically, two behaviors are observed: the charge can rapidly go to zero, so revealing the absence of a topological background; otherwise, it reaches, after a short time, a constant value next to an integer, so indicating the presence of background

instantons.

The irrelevant terms in the lattice action adopted - the Symanzik tree-level improved action - make the lattice action calculated on an instanton decrease when its size decreases. As a consequence, an instanton experiences under cooling a progressive shrinking, up to its destruction. The conclusion is that the cooling procedure affects in a certain degree the background topology, cutting off instantons with size smaller than a certain size, depending on the number of cooling steps performed. This number must be big enough to clear off the quantum noise, but not so much to completely erase most of the topological configurations.

B. Heating an instanton

Here, we apply the method suggested by Teper [3] and already realized in [4] [9], for the determination of $Z(\beta)$. Our contribution is an improvement of the statistic with the purpose to reveal eventual discrepancies from the two-loops perturbative calculation; moreover, we study of the onset of small instantons over the starting topological background.

We put an instanton of charge $Q_0 = 1$ and size 20 lattice units, in the middle of a 120×120 lattice. Starting from this configuration, we construct the ensembles $\{C_t\}$ performing t sweeps of a standard heat-bath algorithm, and measure the average topological charge over each ensemble $\{C_t\}$.

In Fig. 2 we present the results for three different values of β . We observe that a plateau is reached after about 11 heating steps. The independence from β of the starting point of the plateaux has been observed also in previous works: it reveals that $Z(\beta)$ takes its origin from fluctuations of small size, whose thermalization does not undergo critical slowing down.

In Table II we compare $Z(\beta)$ calculated at two loops with the non-perturbative estimate obtained by fitting values at the plateaux. We attribute the small discrepancy to further terms of the perturbative expansion of $Z(\beta)$: a fit gives $z_3 = 0.097(8)$ and

$z_4 = -0.422(12)$, $\chi^2/\text{d.o.f.} = 0.15$.

In order to check the extent of small instantons production during heating, we have analyzed a sample of 1000 configurations obtained after 15 heating steps at $\beta = 1.45$, where the small instantons contamination is expected to be the largest among the values of β considered. We classify each configuration assigning it to a definite topological sector according to its cooled charge. We find that ~ 30 configurations have left the $Q = 1$ sector: ~ 20 migrating into the zero charge sector, and ~ 10 into the $Q = 2$ sector. This effect is to be attributed to the generation of small-size instantons (of charge -1 and $+1$ respectively), laying on the background topological configuration. We explain the small asymmetry observed as the effect of the explicit breaking of the charge symmetry by the starting configuration: starting from the $Q = 1$ sector, it is energetically more convenient to fall into the $Q = 0$ sector than to rise into the $Q = 2$ sector. We have verified that the systematic error induced on the determination of $Z(\beta)$ by a topological contamination of the observed extent is negligible within the statistical uncertainty of our result.

C. Heating the flat configuration

Here, in addition to the standard heat-bath algorithm, we use a faster local algorithm of thermalization, the overheat-bath [9].

First of all, we have analyzed the thermalization process during heating. We have observed the behavior under heating of ξ_{\perp} , the correlation length of the components of the spins orthogonal to the direction of polarization of the starting flat configuration; with this choice we get rid of the effects of $O(3)$ symmetry breaking of the starting configuration.

We have used the following definition [19]:

$$\xi_{\perp}^2 = \frac{1}{4 \sin^2(\pi/L)} \left[\frac{\tilde{G}_{\perp}(0,0)}{\tilde{G}_{\perp}(0,1)} - 1 \right], \quad (16)$$

where

$$\tilde{G}_\perp(k) = \frac{1}{L^2} \sum_{x,y} \langle \phi_\perp(x) \cdot \phi_\perp(y) \rangle \exp \left[i \frac{2\pi}{L} (x - y) \cdot k \right] . \quad (17)$$

We have verified that this quantity reproduces at thermal equilibrium the value ξ_{eq} obtained with the standard definition. In Figs. 3, 4 we present some values of ξ_\perp^2 versus t , the number of heating steps performed, obtained with the two algorithms of thermalization. We observe that the expected law $\xi_\perp^2(t) = ct$ fits data nicely, with $c_h = 0.335 \pm 0.042$, $\chi^2/\text{d.o.f.} \sim 0.01$, for the heat-bath, and $c_{ov} = 1.89 \pm 0.16$, $\chi^2/\text{d.o.f.} \sim 0.79$, for the overheat-bath. We note that the overheat-bath is about six times faster than the heat-bath.

In $SU(2)$ Yang-Mills theory, topological fluctuations are decoupled from the ordinary fluctuations as for thermalization time. This property allows the observation, during the heating of χ^L starting from the flat configuration, of an extended plateau corresponding to the non-topological contribution to χ^L , i.e. the mixing with the identity operator plus the mixing with the gluon condensate [6]. Should this hold also in the $O(3)$ σ model, a plateau in correspondence to $P(\beta)$ would be detectable, and, as a result, a non-perturbative evaluation of such quantity could be obtained - the mixing term is here negligible.

We have performed, at various values of β , measures of χ^L during the heating of the flat configuration with the slower algorithm of thermalization, the standard heat-bath, each ensemble $\{C_t\}$ containing from 10000 to 40000 configurations. Unfortunately, we could not clearly single out any plateau, always obtaining a steady drift to the equilibrium value (see Fig. 5). The situation is the same when the overheat-bath is used, with a six scale factor on the times of thermalization.

Being aware of the ultraviolet nature of the model in study, the explanation of this behavior is straightforward: small-size instantons are precociously generated by the heating algorithm.

In order to check this diagnosis, we systematically cool ensembles $\{C_t\}$, obtained with a standard heat-bath, at values of t beyond the thermalization time of the perturbative fluctuations indicated by the previous works on this matter [4] [9]. We find that five

steps of unconstrained cooling are sufficient to unmask the topological content of the configurations through the observation of the behavior of the topological charge. If cooling is further protracted a part of instantons - the smaller ones - are destroyed: this phenomenon is revealed by the behavior of the charge under cooling that, after a short plateau at a value near to an integer, goes to zero in few steps. The result is that, as expected, the presence of topological fluctuations is relevant already at the first steps of the heating process: the argument that instantons are subject to a special kind of critical slowing down, more severe than non-topological fluctuations, seems not to apply to this model.

Now, if topological configurations are systematically removed from the statistical ensembles $\{C_t\}$, and χ^L is averaged only over the trivial configurations, a long plateau should be observed after the thermalization of the perturbative modes. This plateau would correspond *just* to $P(\beta)$ as defined in Eq. (14).

In order to get rid of instantons, we systematically discard all configurations having, after 5 steps of unconstrained cooling, a topological charge greater than a fixed threshold value. An analysis at $\beta = 1.45$ on a sample $\{C_{70}\}$ consisting of 100 configurations shows that this procedure eliminates almost all configurations with non-trivial topology. In Fig. 6 we show the results obtained at $\beta = 1.45$ for a chosen threshold: a clear long plateau is now observed. We have checked that data are stable under a small change of the threshold: this ensures that the plateau observed is a real effect and not an artifact of the subtraction procedure. We have repeated the above procedure for other values of β : a plateau is observed for $t \geq \bar{t} \simeq 35$, not depending on β as expected; \bar{t} is the time of thermalization of fluctuations with size $l \simeq 4$ lattice spacings which, within our error bars, saturate the perturbative signal, $P(\beta)$. We observe that $P(\beta)$, in comparison with $Z(\beta)$, is sensitive to larger size fluctuations: an indication of this could already be taken out from the perturbative series of $P(\beta)$, which starts to get contribution from higher orders in $1/\beta$. In Table III values of $P(\beta)$ fitted on the plateaux, $P_{np}(\beta)$, are compared with those of $P_{pert}(\beta)$. The latter quantity is obtained in Ref. [9] by a perturbative calculation combined with a fit on $\chi^L(\beta)$ at large β : in this region, the probability

of occurrence of instantons is exponentially suppressed, as well the non-perturbative contribution of other origins, so $P_{pert}(\beta)$ is in all equivalent to a truncated perturbative determination of $P(\beta)$. The agreement observed in Table III reveals that $P(\beta)$ is a substantially perturbative quantity, well approximated by the first few perturbative terms. This result is not trivial, since in $O(N)$ σ models perturbative series are not Borel-summable [20].

Correlations between measures have been taken into account performing standard binning procedures; we observe in this regard that instantons, which are the main source of correlations for χ^L , have been rejected from the ensemble, and so the problem of correlations is less critical than usual.

In order to study the approach to thermal equilibrium of χ^L during the heating of the flat configuration, we exploit the faster overheat-bath algorithm. In Fig. 7 we show the behavior of χ^L during the heating at $\beta = 1.45$: the time required to reach the equilibrium value is consistent with $t_{eq} = \xi_{eq}^2/c_{ov}$. This observation is confirmed, within our error bars, for other values of β . The suggestion we get from this evidence is that instantons undergo the ordinary slowing down: the time of thermalization of all fluctuations depends only on their size - no matter of their topology.

We further observe that the time χ^L takes to overcome its perturbative value (see Fig. 8 and Table III) is the same for different values of β . By a measure at $\beta = 2.50$, we have verified that this is just the time the algorithm takes to thermalize the perturbative fluctuations. The observed time ($\bar{t} \simeq 8$ heating steps) corresponds, according to the random walk law, to thermalized lengths of ~ 4 lattice spacings, in agreement with the results obtained with the heat-bath algorithm. The suggestion is that there is no non-perturbative contribution to χ^L before perturbative modes are thermalized; otherwise, such non-perturbative contribution would give an additional boost to the signal, making it to overcome the perturbative threshold in advance at small β in comparison with the time taken at $\beta = 2.50$ to saturate the perturbative signal.

D. Small instantons size distribution

On the basis of the results of the previous subsection, we make the following work hypothesis about the process of thermalization of topological fluctuations: we assume that the heating algorithm reproduces on the lattice at the time t the equilibrium size distribution of the average instanton number $dN/d\rho$, up to the length thermalized at that t , $l(t)$; we moreover assume that the quantity $\xi_{\perp}(t)$, defined in (16), is a measure of $l(t)$. In this hypothesis, the thermalized length obeys the law $l(t) = \sqrt{ct}$, where c is the same constant that enters the random walk law for ξ_{\perp} and that has been estimated for the two algorithms of thermalization in the previous subsection. Now, called $N(t)$ the average number of instantons in the ensemble at the time t , we write

$$N(t) = \int^{l(t)} d\rho \frac{dN}{d\rho} . \quad (18)$$

In the hypothesis of non-interacting instantons, the average number of instantons in the statistical ensemble, N , is simply related to the topological susceptibility: $\chi = N/V$. Indeed, denoting with $n(\bar{n})$ the number of (anti-)instantons, and with $P_{n,\bar{n}}$ the probability to have a configuration with n instantons and \bar{n} anti-instantons, the following relations hold

$$\chi \equiv \frac{1}{V} \sum_{n,\bar{n}} (n - \bar{n})^2 P_{n,\bar{n}} = \frac{1}{V} \sum_{n,\bar{n}} (n + \bar{n}) P_{n,\bar{n}} \equiv \frac{N}{V} . \quad (19)$$

The hypothesis of non-interacting instantons plays a role in the second equality of (19) since, in this case,

$$P_{n,\bar{n}} = \frac{1}{2^{n+\bar{n}}} \frac{(n+\bar{n})!}{n! \bar{n}!} P_{n+\bar{n}} \quad (20)$$

(P_N is the probability of a configuration with N topological objects, instantons or anti-instantons). We note, by the way, that the above condition is satisfied if $P_{n,\bar{n}} = P_n P_{\bar{n}}$ with $P_{n(\bar{n})}$ poissonian, as in the semiclassical approximation.

Eq. (19), when translated on the lattice in the framework of the field theoretical method, allows to obtain a measure of the average number of instantons in the ensemble $\{C_t\}$, $N(t)$, from the measure of χ^L :

$$\frac{N(t)}{L^2} = \frac{\chi^L(\beta) - P(\beta)}{Z^2(\beta)} \Big|_t \equiv \chi_{np}^L \Big|_t . \quad (21)$$

So, we are in a position to check our hypothesis (18): in Fig. 9 we show $N_\chi(t)$ as obtained from (21) at $\beta = 1.45$ together with the curve obtained from (18) with the choice $dN/d\rho = A/\rho^{1.65}$: we observe that the behavior of $N(t)$ is nicely reproduced.

The average number of instantons in the ensemble at time t can be directly obtained - without passing through χ^L - from the analysis of the frequency of occurrence of configurations in the various topological sectors. Indeed, from the hypothesis of non-interacting instantons, it follows (see (19)):

$$N = \sum_Q Q^2 P_Q . \quad (22)$$

In order to assign each configuration to its topological sector Q , we exploit the above described cooling procedure.

In Fig. 10 we show the behavior of $N_Q(t)$ so obtained at $\beta = 1.45$. We see that $N_Q(t)$ is ~ 0 for $t \leq 2$ heating steps, corresponding to instantons of size ~ 2 lattice spacings: instantons smaller than this size do not survive the cooling process.

For $2 \leq t \leq \bar{t}$ (\bar{t} is the time of thermalization of perturbative fluctuations, corresponding to ~ 4 lattice spacings), $N_Q(t)$ is different from zero even if χ^L has yet no non-perturbative contribution, as observed in the previous subsection. We conclude that instantons with size lower than ~ 4 lattice spacings - though present in the ensembles $\{C_t\}$ - give no non-perturbative contribution to χ^L , so having the same effect of perturbative fluctuations.

For $t \geq \bar{t}$, $N_Q(t)$ is systematically greater than $N_\chi(t)$: this discrepancy is simply explained, since χ^L loses the part of the topological contribution coming from instantons with sizes ranging from ~ 2 to ~ 4 lattice spacings. In formulae:

$$N_\chi(t) = \int_{\sim 4}^{l(t)} d\rho \frac{dN}{d\rho} , \quad (23)$$

while

$$N_Q(t) = \int_{\sim 2}^{l(t)} d\rho \frac{dN}{d\rho} . \quad (24)$$

The mismatch is expected to be just

$$\int_{\sim 2}^{\sim 4} d\rho \frac{dN}{d\rho} \simeq N_Q(\bar{t}), \quad (25)$$

for all $t \geq \bar{t}$. We find that the quantity $N_Q(t) - N_\chi(t)$ is well fitted by a constant ($\chi^2/\text{d.o.f} \sim 0.1$) whose value is consistent with the prevision (25) - see Fig. 11. The same happens at $\beta = 1.525$.

On the basis of the assumption (18) on the mechanism of thermalization of instantons during heating, we can extract from the lattice the size distribution of instantons in the physical vacuum, $dN/d\rho$. Indeed, from Eq. (18) it follows

$$\left. \frac{dN}{d\rho} \right|_{\rho=l(t)} = \frac{1}{dl(t)/dt} \left(\frac{dN}{dt} \right). \quad (26)$$

In Fig. 12 we plot $dN_Q/d\rho$ and $dN_\chi/d\rho$ versus ρ at $\beta = 1.45$ as obtained from Eq. (26). We find that the two determinations of $dN/d\rho$ nicely overlap. The same is done in Fig. 13 at $\beta = 1.525$; data at $\beta = 1.525$ have a suppression $\propto a^3$ in comparison with data at $\beta = 1.45$, since $dN/Vd\rho$ is a renormalization group invariant quantity when V and ρ are measured in physical units.

In Fig. 14 we collect all our data for $dN/Vd\rho$ expressing all quantities in physical units. Data coming from different values of β , covering a spectrum of ρ ranging from 0.2 to 0.9 units of the inverse mass gap, dispose within statistical fluctuations along the same curve, as expected. A global fit with a function A/ρ^n shows that n from 1 to 2 is consistent with data. In fact, n seems to increase with ρ : initial data give $n \simeq 1.5$, while data at $\rho \geq 0.4$ give $n \simeq 2$. This behavior is intermediate to the expectation $n = 1$, from semiclassical prediction at small sizes, and the result $n = 3$ recently obtained in [21], where $dN/Vd\rho$ is determined with different techniques in the region $1 \leq \rho \leq 5.5$. These results seem to suggest for $dN/Vd\rho$ an ever more severe suppression as ρ increases.

Up to the sizes investigated by our analysis ($\rho \simeq 0.2$ inverse mass gap units), no physical ultraviolet cut-off has been observed in the instanton size distribution. Due to this ultraviolet dominance, χ_{np}^L loses a noticeable part of the non-perturbative contribution, if the discretization is too coarse: we argue that this is in fact the case for the

values of β of the numerical simulations up to now performed. Since the amount of the lost contribution decreases as β increases, a scaling defect for χ_{np}^L should be observed. In the following, we show the results of $\chi_{np}^L/f^2(\beta)$ at thermal equilibrium for three values of β in the expected scaling region; $f(\beta) = 2\pi\beta e^{-2\pi\beta}$ is the two-loop renormalization group function and χ_{np}^L has been obtained from standard Monte Carlo simulations using the non-perturbative determinations of $P(\beta)$ and $Z(\beta)$:

$$\begin{aligned}
\beta = 1.45 & : & 196 \pm 11 & & (27) \\
\beta = 1.50 & : & 224 \pm 13 & & \\
\beta = 1.525 & : & 250 \pm 14 & . &
\end{aligned}$$

The increasing behavior observed indicates that, for the values of β in study, χ_{np}^L has not yet saturated all topological contributions.

V. CONCLUSIONS

In this paper we have studied the behavior of topological small-size fluctuations under heating in the $O(3)$ σ model. The main conclusion is that small instantons undergo ordinary slowing down: instantons with a given size reach the thermodynamical equilibrium distribution when the heating algorithm attains the corresponding length. A different conclusion in this regard is settled in $SU(2)$ Yang-Mills theory, where instantons are believed to undergo a form of critical slowing down more severe than ordinary fluctuations. We think that this state of things is to be attributed to the pathological characteristic of the topology in the $O(3)$ σ model, exhibiting ultraviolet dominance.

As a by-product of the present work, we have obtained a high-precision non-perturbative estimate of the mixing of the lattice topological susceptibility with the unity operator, finding good agreement with perturbative results. This shows that this quantity is essentially perturbative. We have also obtained the size distribution function of the average number of instantons in the physical vacuum in a region of sizes not yet explored, reaching sizes of a small fraction of the inverse mass gap, the physical length

of the model. These results lay on a two-fold assumption: first, instantons thermalize as ordinary fluctuations; second, instantons do not interact among themselves. The first assumption is consistent with other results of the present work; the second is reasonable if one takes into account that the typical sizes of instantons involved in our analysis are much smaller than the lattice size.

Up to the sizes explored, no physical cut in the distribution function has been observed, so having a new evidence that the topology of the $O(3)$ σ model is strongly ultraviolet dominated. Moreover, we have found that the lattice-regularized version of the topological susceptibility has a non-physical cut-off in the size of instantons corresponding to ~ 4 lattice spacings. As a consequence, a part of the non-perturbative contribution to the topological susceptibility is lost on the lattice, at least in the region of β up to now explored in numerical simulations. We attribute to this loss of non-perturbative signal - decreasing as β increases - the observed deviation from scaling of the topological susceptibility on the lattice.

We have also argued on the basis of a perturbative calculation, that the mixing of the lattice topological susceptibility with the action density is a negligible part of the total non-perturbative signal.

The ultimate consideration of this work is a caveat: when the $O(3)$ σ model is used as a laboratory to get insight into methods conceived for the theory of physical interest, i.e. QCD , the possibility to be wrecked in the unphysical artefacts of the model must be seriously considered.

Acknowledgements. We wish to thank Adriano Di Giacomo for having suggested the problem, Massimiliano Ciuchini, Paolo Rossi and Ettore Vicari for many useful and stimulating conversations.

APPENDIX

Calculation of the mixing coefficient

For both continuum and lattice calculations at low temperatures, the perturbative expansion is obtained by setting $\phi \equiv [\pi_i, \sqrt{1 - \sum_i \pi_i^2}]$, $i = 1, 2$. The perturbation theory suffers from infrared divergences, which can be cured by adding a magnetic term to the action

$$S_M = \int d^2x h \sqrt{1 - \sum_i \pi_i^2} . \quad (28)$$

Indeed, S_M explicitly breaks the $O(3)$ invariance and acts as a mass term for the π field. The $O(3)$ invariant quantities (and the relations among them) are free of infrared divergences, and have a well-defined limit for $h \rightarrow 0$.

From the standard theory of the renormalization of composite operators it follows that the coefficients $Z(\beta)$ and $A(\beta)$ enter the relation

$$\Gamma_{[\sum_x Q^L(x)Q^L(y)], ren}^{(n)} = a^2 Z(\beta)^2 \Gamma_{[\int_x Q(x)Q(y)], ren}^{(n) (\overline{MS})} + a^2 A(\beta) \Gamma_{[S(y)], ren}^{(n)} + O(a^4) \quad , \quad (29)$$

where $\Gamma_{[O], ren}^{(n)}$ stands for n -point ($n \neq 0$) renormalized Γ -function with the insertion of the operator O and \overline{MS} is an arbitrarily chosen renormalization scheme. Eq. (29) allows to calculate $A(\beta)$, order by order in perturbation theory, as a series in $1/\beta$: $A(\beta) = \sum_n a_n/\beta^n$. In Eq. (29), an integration over the variable y is allowed since there are no operators other than $S(x)$ with the same quantum numbers of χ (this would be forbidden in the case of mixings with several operators differing by an integration by parts). After the integration, Eq. (29) becomes

$$\Gamma_{[(Q^L)^2/V], ren}^{(n)} = Z(\beta)^2 \Gamma_{[Q^2/V], ren}^{(n) (\overline{MS})} + A(\beta) \Gamma_{[S(0)], ren}^{(n)} + O(a^2) \quad , \quad (30)$$

where $V = L^2 a^2$ is the space-time volume. Now the vertices of the topological charge appear in the diagrams at zero momentum, with a considerable simplification of the calculation.

In view of a perturbative evaluation of $A(\beta)$, the most suitable choice is $n = 2$, with an insertion of two external lines of the field π with the same index i . At the lowest order:

$$\Gamma_{[S(0)], ren}^{(2)} = 2p^2 \quad , \quad (31)$$

where p is the momentum flowing in the external lines, and there is only one diagram \mathcal{D} - order $1/\beta^3$ - contributing to $\Gamma_{[Q^2/V]}^{(2)}$, both on the lattice and on the continuum (Fig. 1). A straightforward calculation shows that the diagram vanishes on the continuum: $\mathcal{D}|_{cont} = 0$. As a consequence:

$$\mathcal{D}|_{latt} = \frac{a_3}{\beta^3} 2p^2 + O(a^2) \quad ; \quad (32)$$

a_3 is just the coefficient we are looking for.

We now present the complete calculation of $\mathcal{D}|_{latt}$. All the results will be expressed as obtained in the infinite-size lattice: they can be translated in the finite-size case by simply interpreting integrals as discrete sums. We first give the explicit expression of the four-legs vertex of the lattice topological charge operator Q^L :

$$\frac{1}{8\pi} \int \Pi_i \frac{d^2 p_i}{(2\pi)^2} V(p_1, p_2) (2\pi)^2 \delta(\sum_i p_i) \pi_1(p_1) \pi_2(p_2) \pi(p_3) \cdot \pi(p_4) \quad , \quad (33)$$

where all the integrations are from $-\pi$ to π , the index i runs from 1 to 4, and

$$V(p_1, p_2) = \epsilon_{\mu\nu} [\sin p_{1\mu} \sin p_{2\nu} - \sin(p_1 + p_2)_\mu (\sin p_{1\nu} - \sin p_{2\nu})] \quad . \quad (34)$$

The result of the diagram in Fig. 1 is:

$$\frac{1}{8\pi^2 \beta^3} \int \frac{d^2 p_1}{(2\pi)^2} \frac{d^2 p_2}{(2\pi)^2} \frac{\mathcal{I}(p, p_1, p_2)}{(\square_{p_1} + h)(\square_{p_2} + h)(\square_{p+p_1+p_2} + h)} \quad , \quad (35)$$

where \square_p is a shorthand for the inverse propagator of the Symanzyk tree-level improved action

$$\begin{aligned} \square_p &= \sum_{\mu} \hat{p}_{\mu}^2 + \frac{1}{12} \sum_{\mu} (\hat{p}_{\mu}^2)^2 \quad , \\ \hat{p}_{\mu}^2 &= \hat{p}_{\mu} \hat{p}_{\mu}^* \quad , \quad \hat{p}_{\mu} = e^{ip_{\mu}a} - 1 \quad , \end{aligned} \quad (36)$$

and $\mathcal{I}(p, p_1, p_2)$ is a compact notation for

$$V(p, p_1)V(p, p_1) + V(p, p_1)V(p, p_2) + 2V(p, p_2)V(p_1, p_2) + (V(p_1, p_2))^2 + V(p_1, p_2)V(p + p_1 + p_2, -p_2). \quad (37)$$

It may be checked that the integral in (35) is convergent in the limit $h \rightarrow 0$. The correct procedure would be now calculating exactly the above integral and extracting the term proportional to p^2 in the result of the integration. A look at the complete expression suffices to discourage any attempt in this direction. The other, apparently viable, possibility of performing Taylor expansions in the integrand and isolating the p^2 term before integration, does not work [22]. We have found a way to get the result without any Taylor expansion, relying only upon the symmetries of the vertex $V(p_1, p_2)$.

Let us consider, for example, the contribution to (35) coming from the third term in (37):

$$\frac{2}{8\pi^2\beta^3} \int \frac{V(p, p_2)V(p_1, p_2)}{(\square_{p_1} + h)(\square_{p_2} + h)(\square_{p+p_1+p_2} + h)} \equiv \frac{1}{8\pi^2\beta^3} \mathcal{I}_3. \quad (38)$$

After the translation $p_1 \rightarrow p_1 - p$ we have

$$\mathcal{I}_3 = 2 \int \frac{V(p, p_2)V(p_1 - p, p_2)}{(\square_{p_1-p} + h)(\square_{p_2} + h)(\square_{p_1+p_2} + h)}. \quad (39)$$

We observe that $V(p, p_2)$ factors out a $\sin p \sim p$ term, while $V(p_1 - p, p_2)$ may be decomposed into $V(p_1, p_2)$ and the remaining part, $V_r(p, p_1, p_2)$, which is $O(p)$. When $V(p, p_2)$ multiplies V_r the p^2 term comes out trivially and it is sufficient to put $p = 0$ in the propagators; the part with $V(p, p_2)V(p_1, p_2)$ reduces to $-\mathcal{I}_3$ after the following transformation of the integration variable p_1 : $p_1 \rightarrow p_1 - p_2$, $p_1 \rightarrow -p_1$ and using the property $V(-p_1 - p_2, p_2) = -V(p_1, p_2)$.

A similar procedure works for the contribution to (35) from the fourth and the fifth terms in (37), while the first and the second terms need no manipulation because the factorization of p^2 is trivial.

The sum of the various terms in (35) after the factorization of $2p^2$ is an IR-convergent integral where h can be safely put equal to zero; the mixing coefficient a_3 we are looking for, is:

$$\frac{1}{16\pi^2} \int \square_{p_1}^{-1} \square_{p_2}^{-1} \square_{p_1+p_2}^{-1} \left\{ \sin^2 p_{1\mu} (2 + \cos p_{1\nu})^2 + \sin p_{1\mu} \sin p_{2\mu} (2 + \cos p_{1\nu})(2 + \cos p_{2\nu}) \right. \\ \left. \sin p_{2\nu} (2 + \cos p_{2\mu}) [(\sin p_{1\nu} - \sin p_{2\nu}) \cos(p_1 + p_2)_\mu - (\sin p_{2\nu} - \sin(p_1 + p_2)_\nu) \cos p_{1\mu}] \right. \\ \left. + \frac{1}{2} [(\sin p_{1\nu} - \sin p_{2\nu}) \cos(p_1 + p_2)_\mu - (\sin p_{2\nu} - \sin(p_1 + p_2)_\nu) \cos p_{1\mu}]^2 \right\} , \quad (40)$$

where there is no sum over repeated indices; μ and ν indicate two different directions.

In Table I we report values of a_3 for various lattices.

In order to evaluate the relevance of the mixing of χ^L with the action density in the determination of χ from lattice simulations, we now need an estimate of the condensate $\langle S(0) \rangle$. The only available result comes from the large N limit [17]:

$$\langle S(0) \rangle|_{N \rightarrow \infty} = -\frac{1}{2N} m^2 . \quad (41)$$

By using the exact relation between the mass gap of the theory, m , and the scale invariant parameter of the lattice Symanzik-improved theory, Λ_{SY} [23], we obtain the estimate for $N = 3$

$$\langle S(0) \rangle \simeq -200 \Lambda_{SY}^2 . \quad (42)$$

This result, combined with our estimate for $A(\beta)$, gives a mixing term which is negligible with respect to the topological non-perturbative signal: at $\beta = 1.45$, for instance, $A(\beta) \langle S(0) \rangle / [Z^2(\beta) \chi] \sim 6 \cdot 10^{-4}$. We believe that higher order corrections in $1/N$ and $1/\beta$ cannot spoil the validity of this argument.

REFERENCES

- [1] M. Campostrini, A. Di Giacomo and H. Panagopoulos, Phys. Lett. **B212** (1988) 206.
- [2] M. Campostrini, A. Di Giacomo, H. Panagopoulos and E. Vicari, Nucl. Phys. **B239** (1990) 683.
- [3] M. Teper, Phys. Lett. **B232** (1989) 227.
- [4] A. Di Giacomo and E. Vicari, Phys. Lett. **B275** (1992) 429.
- [5] M. Campostrini, P. Rossi and E. Vicari, Phys. Rev. **D46** (1992) 4643.
- [6] B. Alles, M. Campostrini, A. Di Giacomo, Y. Gündüç and E. Vicari, Phys. Rev. **D48** (1993) 2284.
- [7] F. Farchioni and A. Papa, Phys. Lett. **B306** (1993) 108.
- [8] A. Di Giacomo and G.C. Rossi, Phys. Lett. **B100** (1981) 692.
- [9] A. Di Giacomo, F. Farchioni, A. Papa and E. Vicari, Phys. Rev. **D46** (1992) 4630; Phys. Lett. **B276** (1992) 148.
- [10] A. Jevicki, Nucl. Phys. **127** (1977) 125;
V.A. Fateev, I.V. Frolov and A.S. Schwarz, Nucl. Phys. **B154** (1979) 1.
- [11] G. 't Hooft, Phys. Rev. Lett. **37** (1976) 8; Phys. Rev. **D14** (1976) 3432.
- [12] A. D'Adda, M. Lüscher and P. Di Vecchia, Nucl. Phys. **B146** (1978) 63.
- [13] A.A. Belavin and A.M. Polyakov, JETP Lett., Vol. 22, No. 10 (1975) 245.
- [14] K. Symanzik, Nucl. Phys. **B226** (1983) 205.
- [15] P. Di Vecchia, K. Fabricius, G. C. Rossi and G. Veneziano, Nucl. Phys. **B192** (1981) 392;
K. Ishikawa, G. Schierholz, H. Schneider and M. Teper, Phys. Lett. **B128** (1983)

- [16] R. J. Crewther, *Nuovo Cimento, Rev. series 3, Vol. 2, (1979) 8.*
- [17] M. Campostrini and P. Rossi, *Phys. Lett.* **B242** (1990) 81.
- [18] M. Teper, *Phys. Lett.* **171** (1986) 81 and 86.
- [19] M. Campostrini, P. Rossi and E. Vicari, *Phys. Rev.* **D46** (1992) 2647.
- [20] S. David, *Nucl. Phys.* **B209** (1982) 433; *Nucl. Phys.* **B234** (1984) 237;
- [21] C. Michael and P.S. Spencer, ‘Instanton size distribution in $O(3)$ ’, Liverpool preprint, LTH 331/94.
- [22] B. Alles and M. Giannetti, *Phys. Rev.* **D44** (1991) 513.
- [23] P. Hasenfratz, M. Maggiore and F. Niedermayer, *Phys. Lett.* **245** (1990) 522.

TABLE I: a_3 for a variety of lattices. a_3 is the first non-vanishing term in the perturbative expansion $A(\beta) = \sum_n a_n/\beta^n$ of the mixing coefficient of the topological susceptibility with the action density. L is the lattice size.

L	$a_3 \times 10^3$	L	$a_3 \times 10^3$	L	$a_3 \times 10^3$
10	0.31450626	60	0.33496730	110	0.33538507
20	0.33022955	70	0.33512505	120	0.33541334
30	0.33318636	80	0.33522745	130	0.33543534
40	0.33422462	90	0.33529767	140	0.33545280
50	0.33470577	100	0.33534790	∞	0.33556212

Table II: $Z(\beta)$ versus β . $Z(\beta)_{2loops}$ is the multiplicative renormalization calculated to two loops. $Z(\beta)_{MC}$ is the multiplicative renormalization calculated by heating an instanton; the size of the lattice is 120; Stat is the statistic of the simulation. Since data on the plateau are correlated, we report the average error of data.

β	$Z(\beta)_{2loops}$	$Z(\beta)_{MC}$	Stat
2.	0.643	0.6285(26)	16000
1.65	0.564	0.5298(42)	16000
1.45	0.500	0.4362(31)	64000

Table III: $P(\beta)$ versus β for different choices of the threshold. $P(\beta)_{pert}$ includes the perturbative tail calculated to four loops and higher order terms fitted from thermal equilibrium Monte Carlo data at large β . $P(\beta)_{np}$ is the perturbative tail calculated by Monte Carlo techniques; the size of the lattice is 120; Stat is the statistic of the simulation.

β	Threshold	$P(\beta)_{pert} \times 10^5$	$P(\beta)_{np} \times 10^5$	Stat
1.45	0.2	5.21(14)	5.24(6)	5000
	0.4		5.26(5)	
	0.6		5.28(6)	
1.50	0.2	4.20(12)	4.22(3)	5000
	0.4		4.23(3)	
	0.6		4.24(3)	
1.525	0.2	3.89(10)	3.82(2)	5000
	0.4		3.83(2)	
	0.6		3.86(2)	
1.55	0.2	3.54(9)	3.50(2)	5000
	0.4		3.51(2)	
	0.6		3.53(2)	

FIGURES

FIG. 1. Diagram contributing to the two-point proper function with insertion of $(Q^L)^2/V$. White crossed blobs indicate the charge operator.

FIG. 2. Q^L versus the heating step. The thermalization is performed by the heat-bath algorithm at $\beta = 1.45, 1.65, 2.00$ on a 120^2 lattice. The solid lines indicate the values of $Z(\beta)$ estimated by averaging data at the plateaux.

FIG. 3. ξ_{\perp}^2 versus the heating step with the heat-bath algorithm at $\beta = 1.45$. The solid line indicates the best fit with the law $\xi_{\perp}^2 = ct$ (with the relative error).

FIG. 4. As in Fig. 5 with the overheat-bath algorithm. Data are obtained at two different values of β : 1.45 and 1.525.

FIG. 5. χ^L versus the heating step at $\beta = 1.45$ starting from the flat configuration on a 120^2 lattice. The thermalization is performed by the heat-bath algorithm. The two solid lines indicate the estimate of $P(\beta)$ by perturbative calculation and the value of χ^L obtained at the thermal equilibrium (with the respective errors).

FIG. 6. χ^L versus the heating step at $\beta = 1.45$ starting from the flat configuration on a 120^2 lattice. The thermalization is performed by the heat-bath algorithm with the procedure of subtraction of topological configurations described in the text. The threshold is 0.4. The solid line indicates the value of $P(\beta)$ estimated averaging data at the plateau (with the relative error).

FIG. 7. The approach to equilibrium of χ^L at $\beta = 1.45$ with the overheat-bath algorithm. The two solid lines are the non-perturbative estimate of $P(\beta)$ and the value of χ^L obtained by standard MC simulations at the thermal equilibrium (with the respective errors).

FIG. 8. The overcoming of the perturbative value during the heating of χ^L at various β . The solid lines are the perturbative values.

FIG. 9. The average number of instantons obtained from χ^L at $\beta = 1.45$ versus the heating step. The solid line represents the predicted behavior in our model of

thermalization (see the text).

FIG. 10. The same quantity of Fig. 9 obtained from the frequency of the configurations in the various topological sectors.

FIG. 11. Comparison of the quantities of Figs. 9 and 10 after the subtraction from data of Fig. 10 of the instantons with sizes smaller than the typical perturbative ranges, which give no contribution to the non-perturbative part of χ^L .

FIG. 12. The instanton size distribution (in lattice units) as obtained from the two methods described in the text, at $\beta = 1.45$.

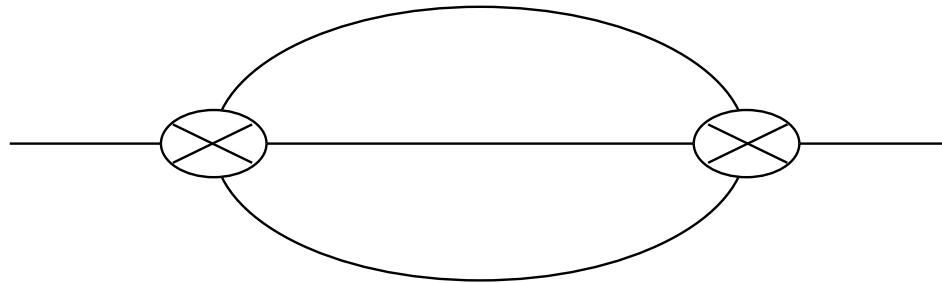
FIG. 13. As in Fig. 12 with $\beta = 1.525$.

FIG. 14. The instanton size distribution in physical units obtained collecting data at different values of β . The solid line is the best fit with $n = 1.5$.

This figure "fig1-1.png" is available in "png" format from:

<http://arxiv.org/ps/hep-lat/9407026v1>

Figure 1



This figure "fig2-1.png" is available in "png" format from:

<http://arxiv.org/ps/hep-lat/9407026v1>

This figure "fig3-1.png" is available in "png" format from:

<http://arxiv.org/ps/hep-lat/9407026v1>

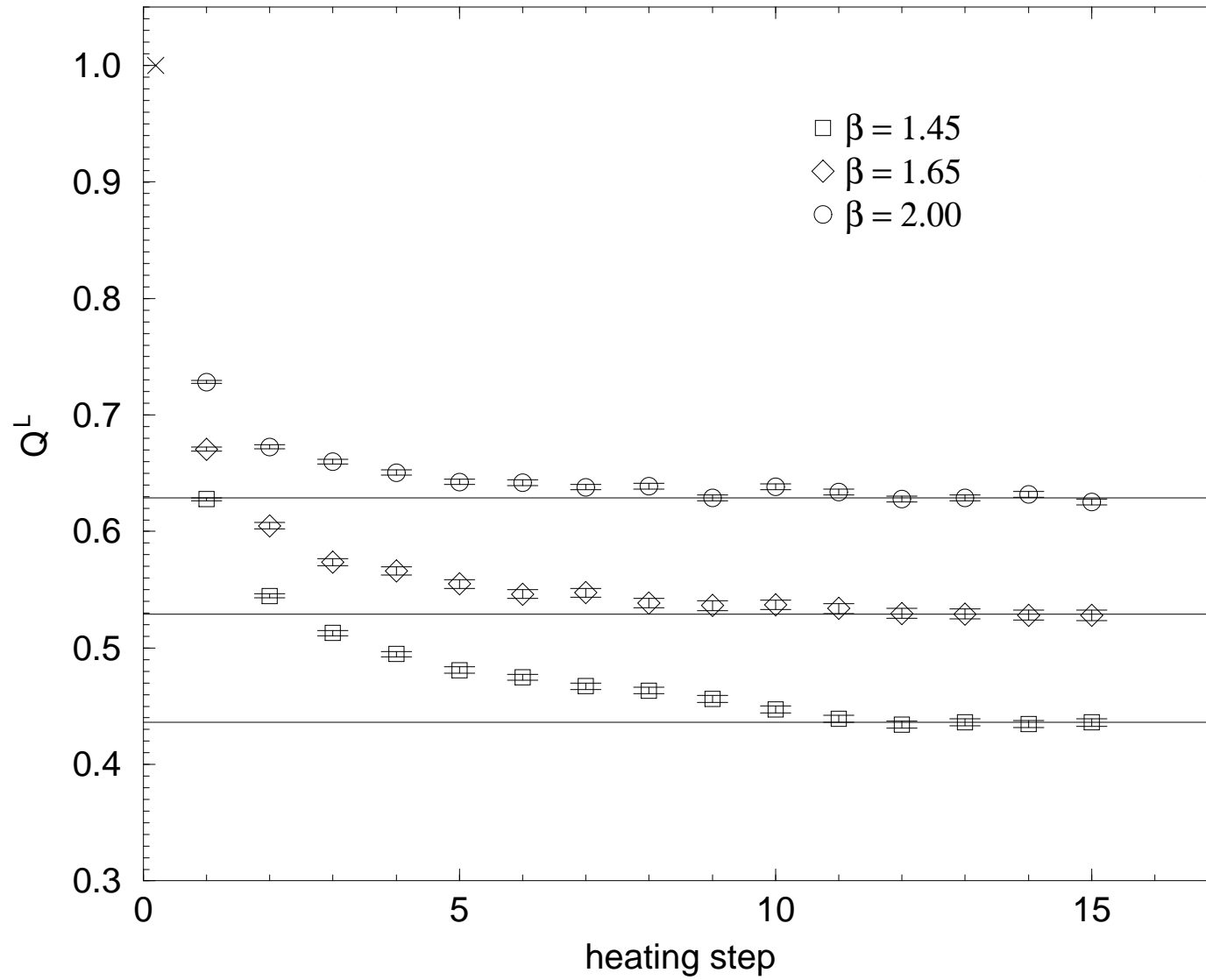
This figure "fig1-2.png" is available in "png" format from:

<http://arxiv.org/ps/hep-lat/9407026v1>

This figure "fig2-2.png" is available in "png" format from:

<http://arxiv.org/ps/hep-lat/9407026v1>

Figure 2



This figure "fig3-2.png" is available in "png" format from:

<http://arxiv.org/ps/hep-lat/9407026v1>

This figure "fig1-3.png" is available in "png" format from:

<http://arxiv.org/ps/hep-lat/9407026v1>

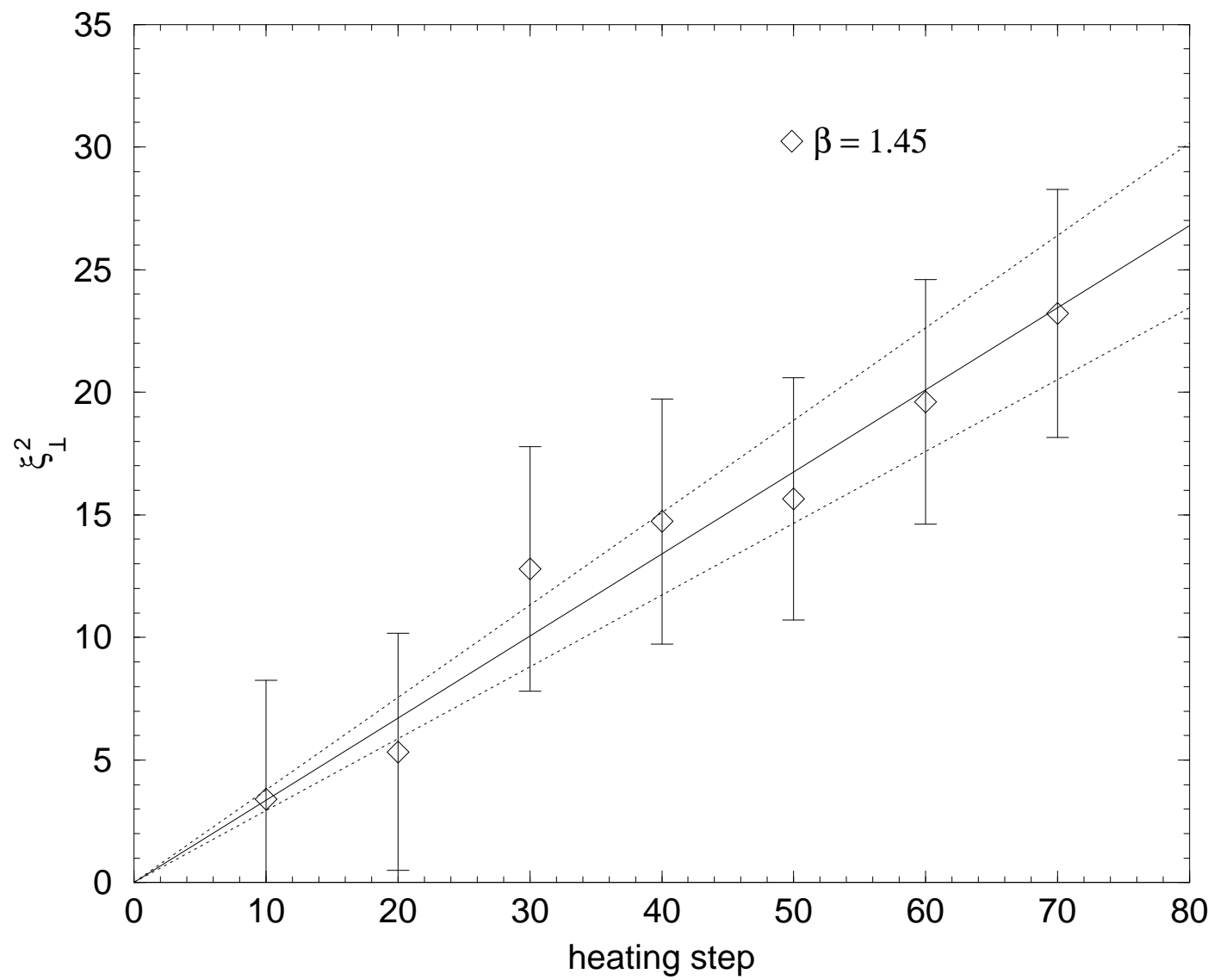
This figure "fig2-3.png" is available in "png" format from:

<http://arxiv.org/ps/hep-lat/9407026v1>

This figure "fig3-3.png" is available in "png" format from:

<http://arxiv.org/ps/hep-lat/9407026v1>

Figure 3



This figure "fig1-4.png" is available in "png" format from:

<http://arxiv.org/ps/hep-lat/9407026v1>

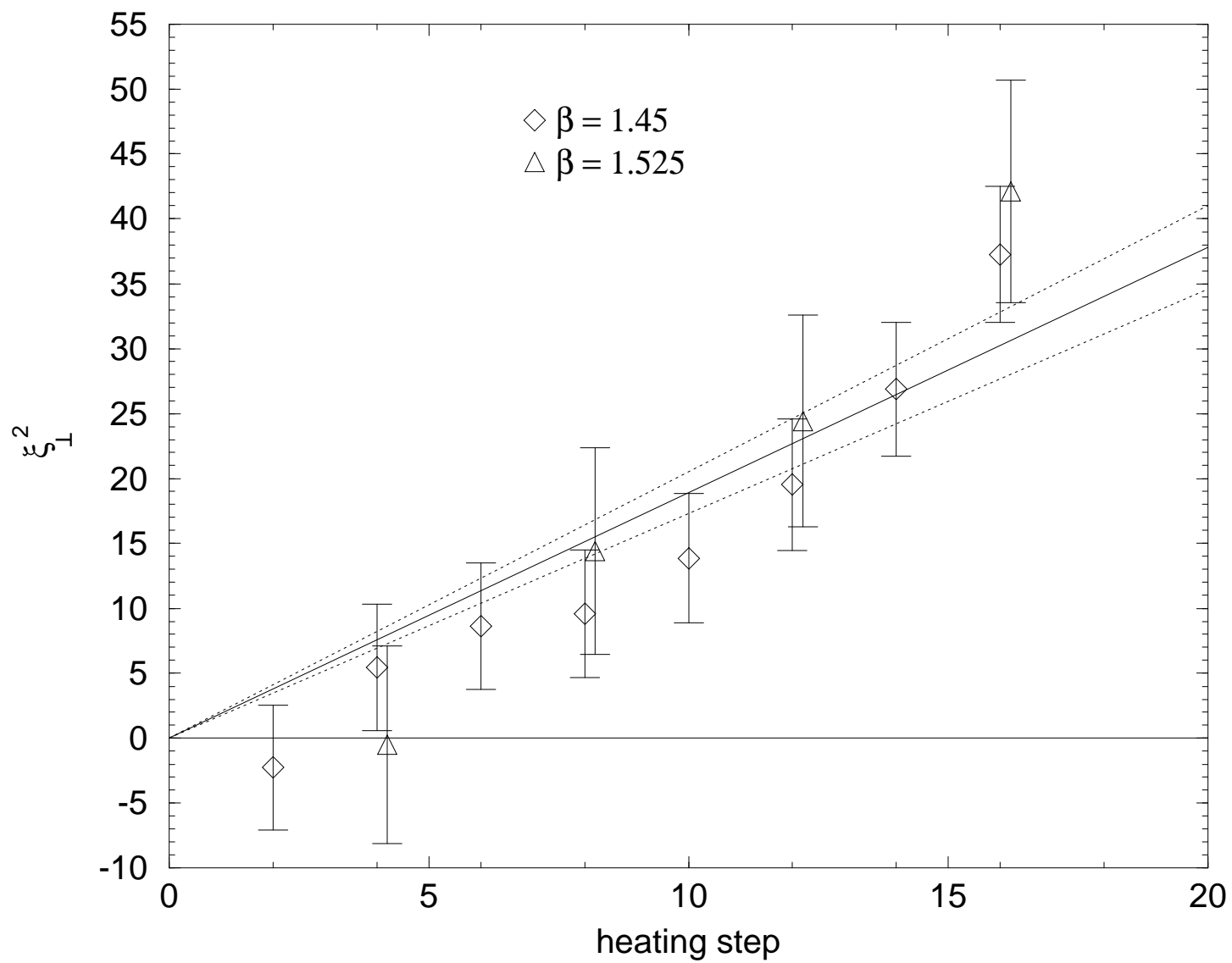
This figure "fig2-4.png" is available in "png" format from:

<http://arxiv.org/ps/hep-lat/9407026v1>

This figure "fig3-4.png" is available in "png" format from:

<http://arxiv.org/ps/hep-lat/9407026v1>

Figure 4



This figure "fig1-5.png" is available in "png" format from:

<http://arxiv.org/ps/hep-lat/9407026v1>

This figure "fig2-5.png" is available in "png" format from:

<http://arxiv.org/ps/hep-lat/9407026v1>

Figure 5

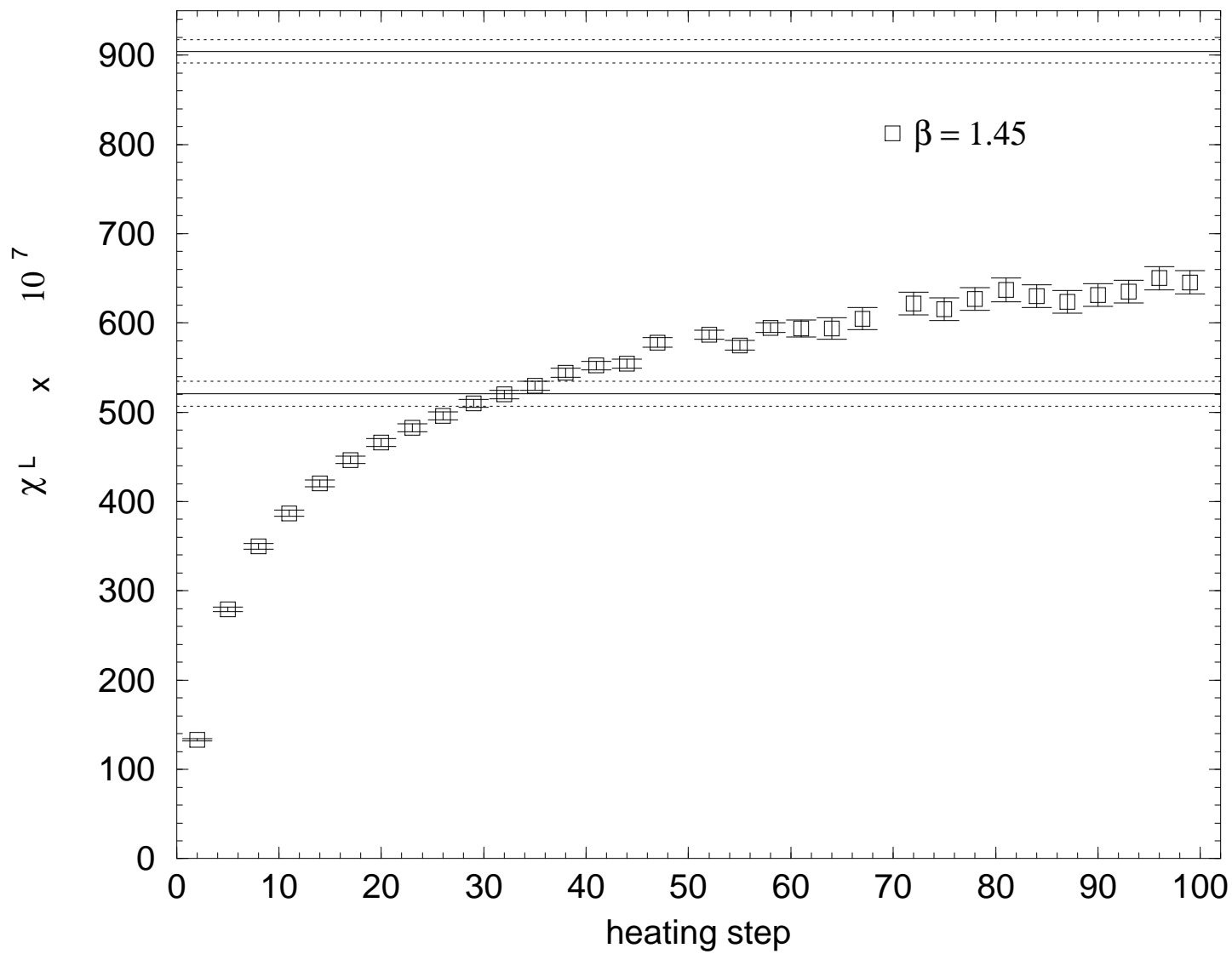


Figure 6

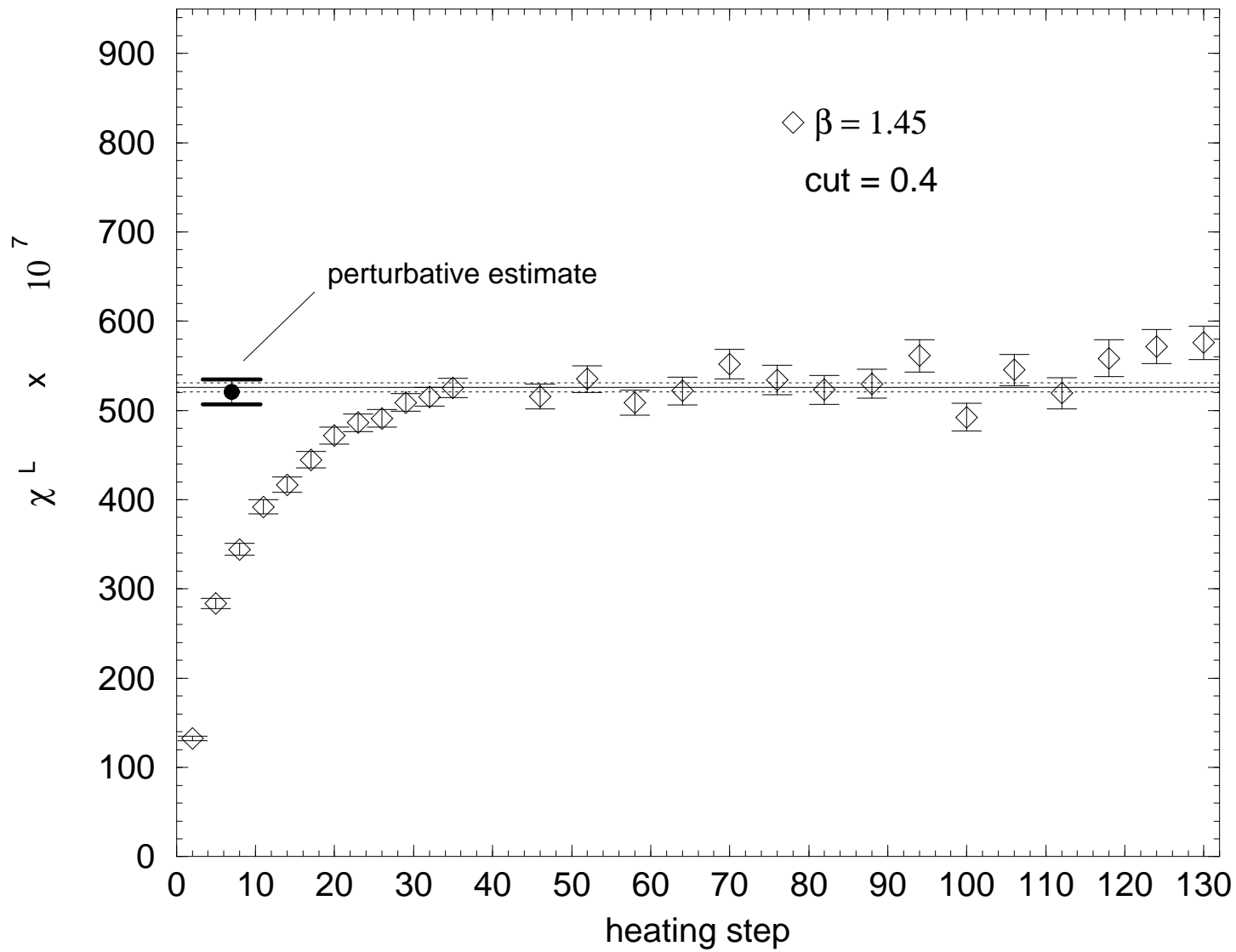


Figure 7

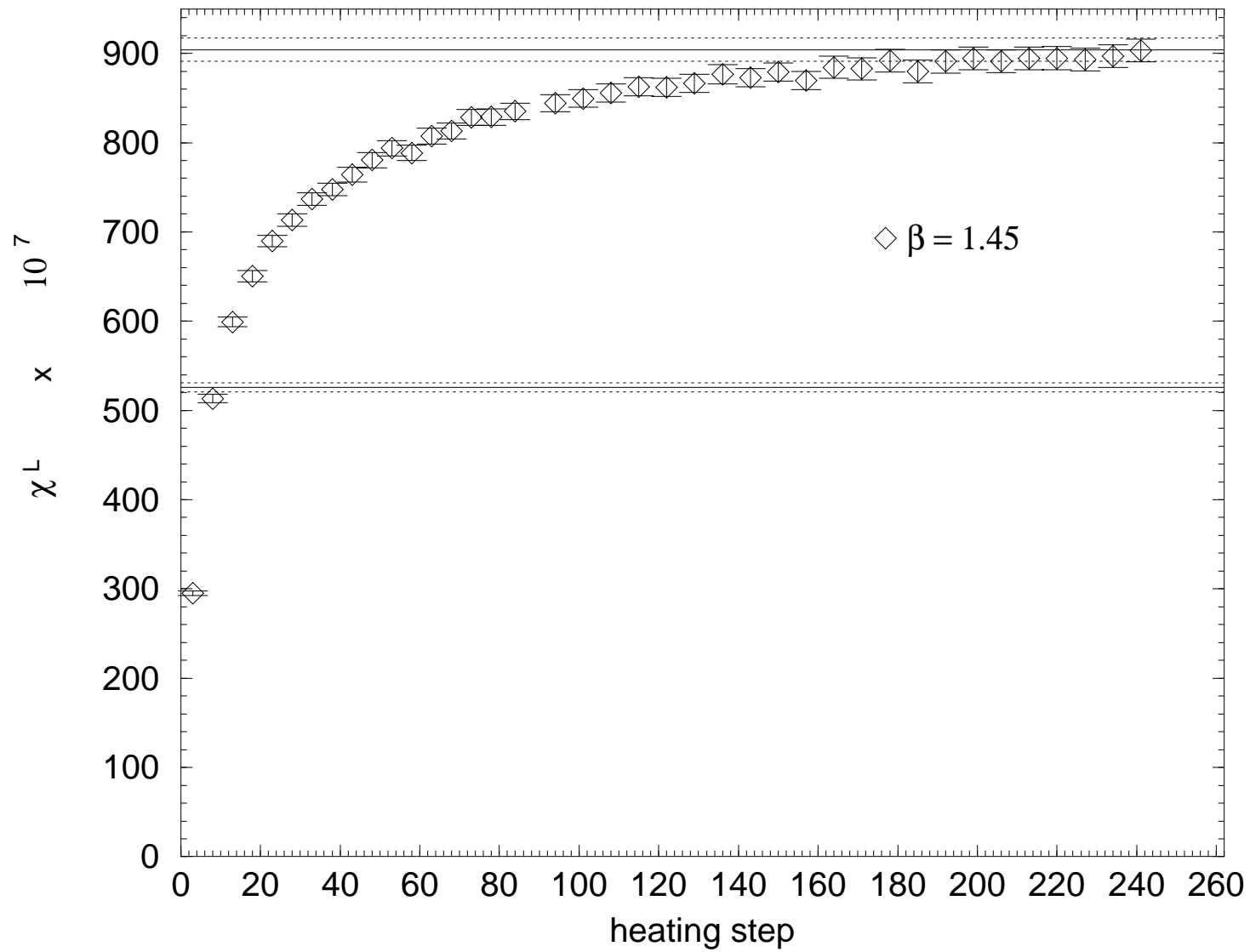


Figure 8

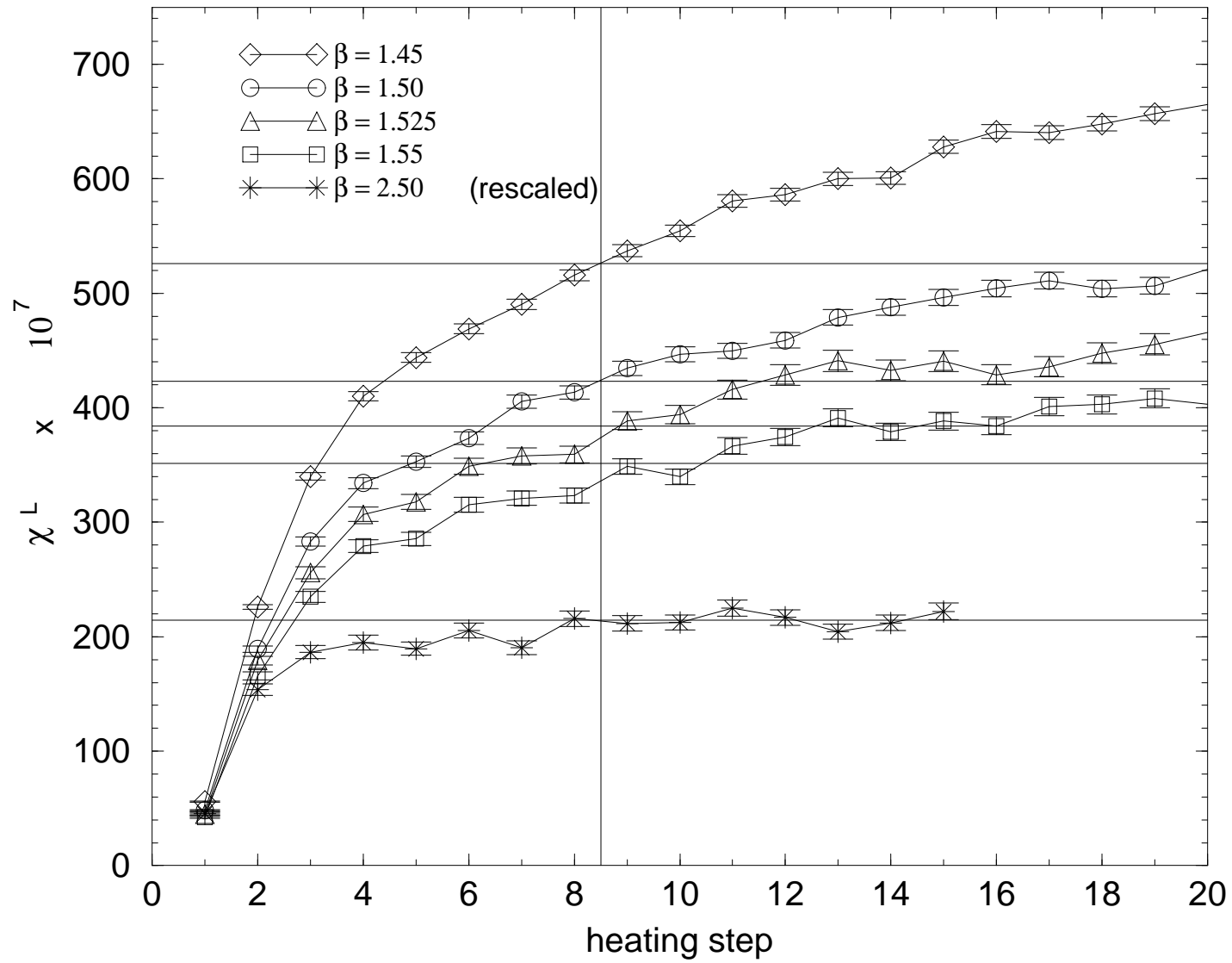


Figure 9

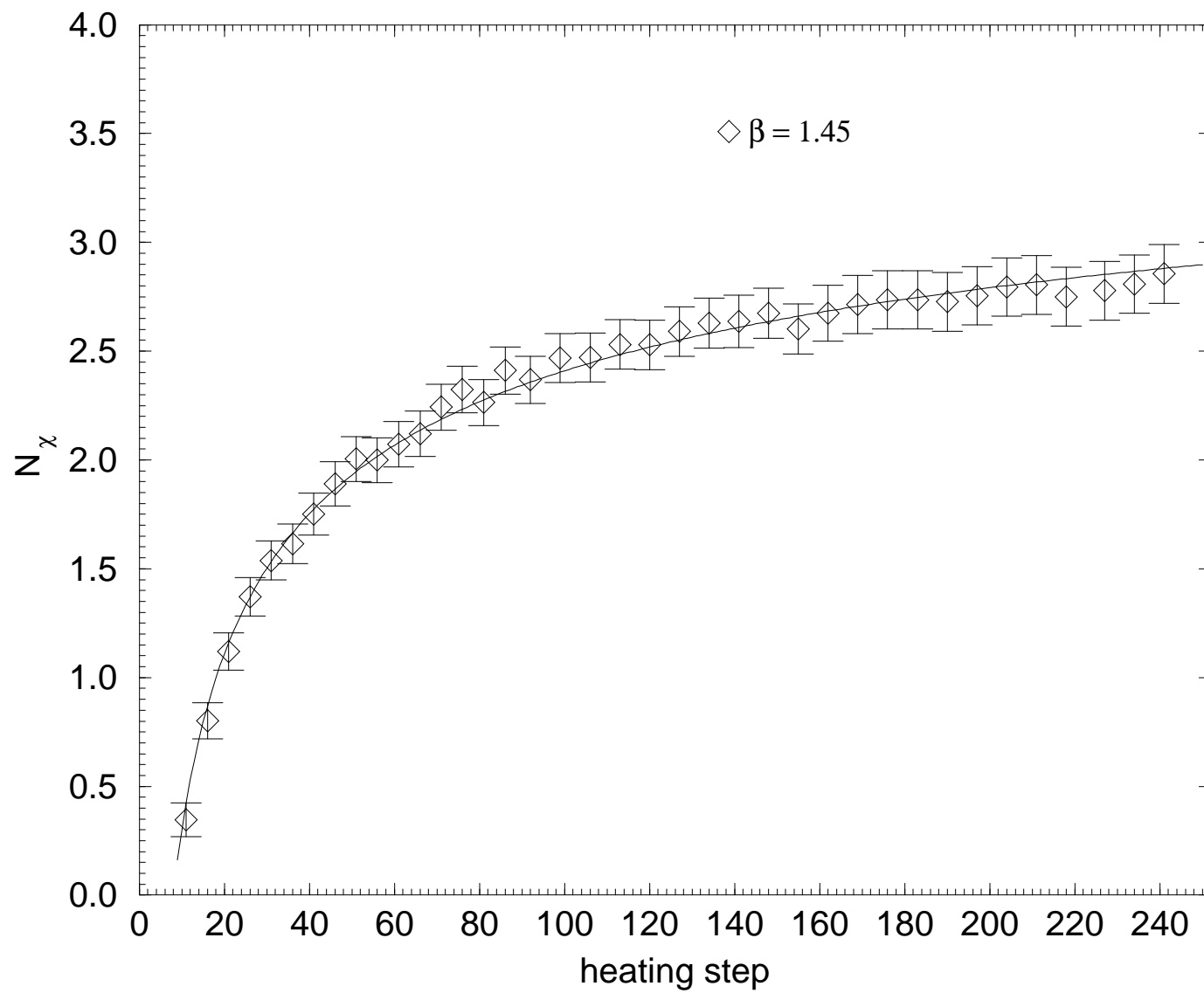


Figure 10

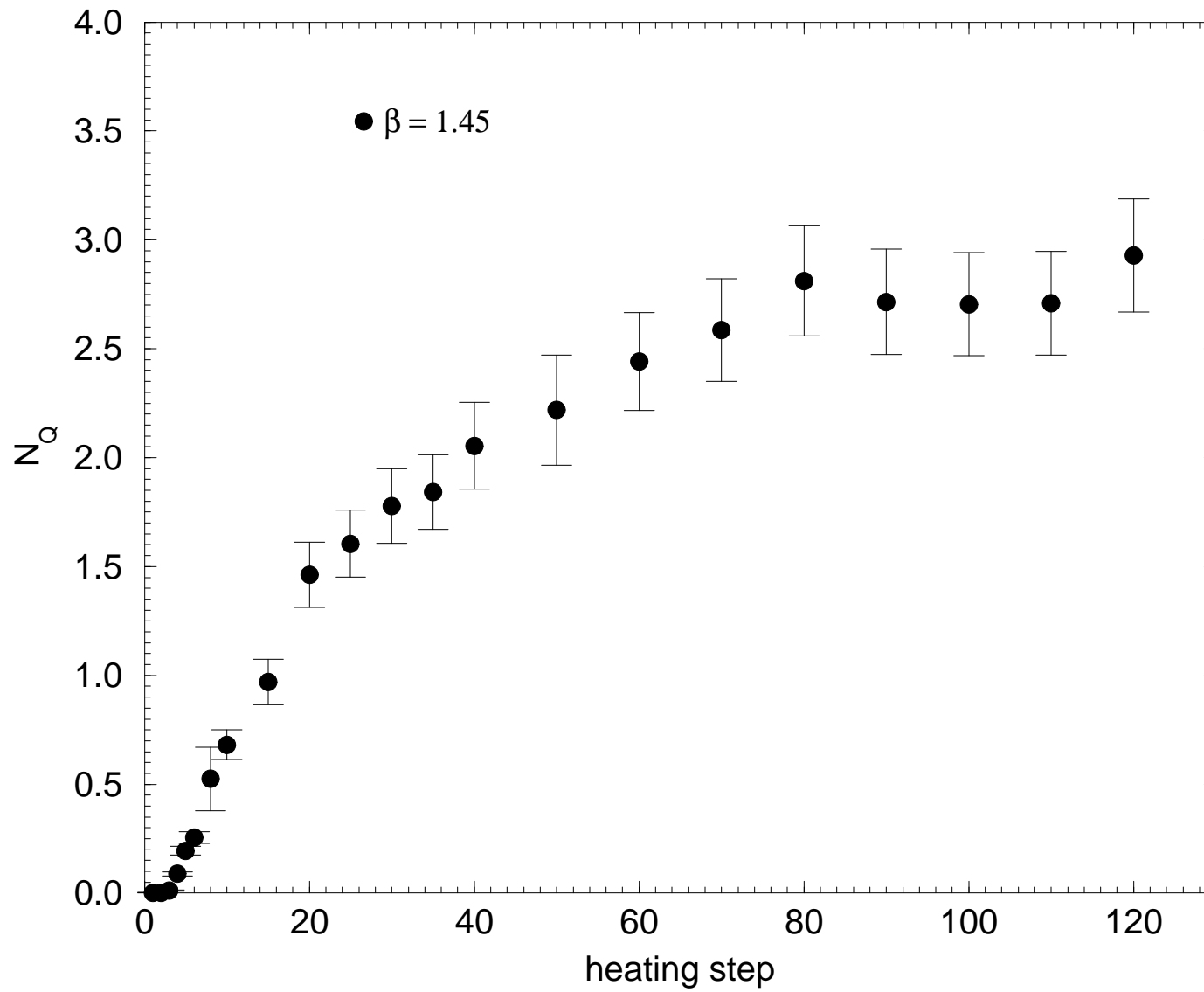


Figure 11

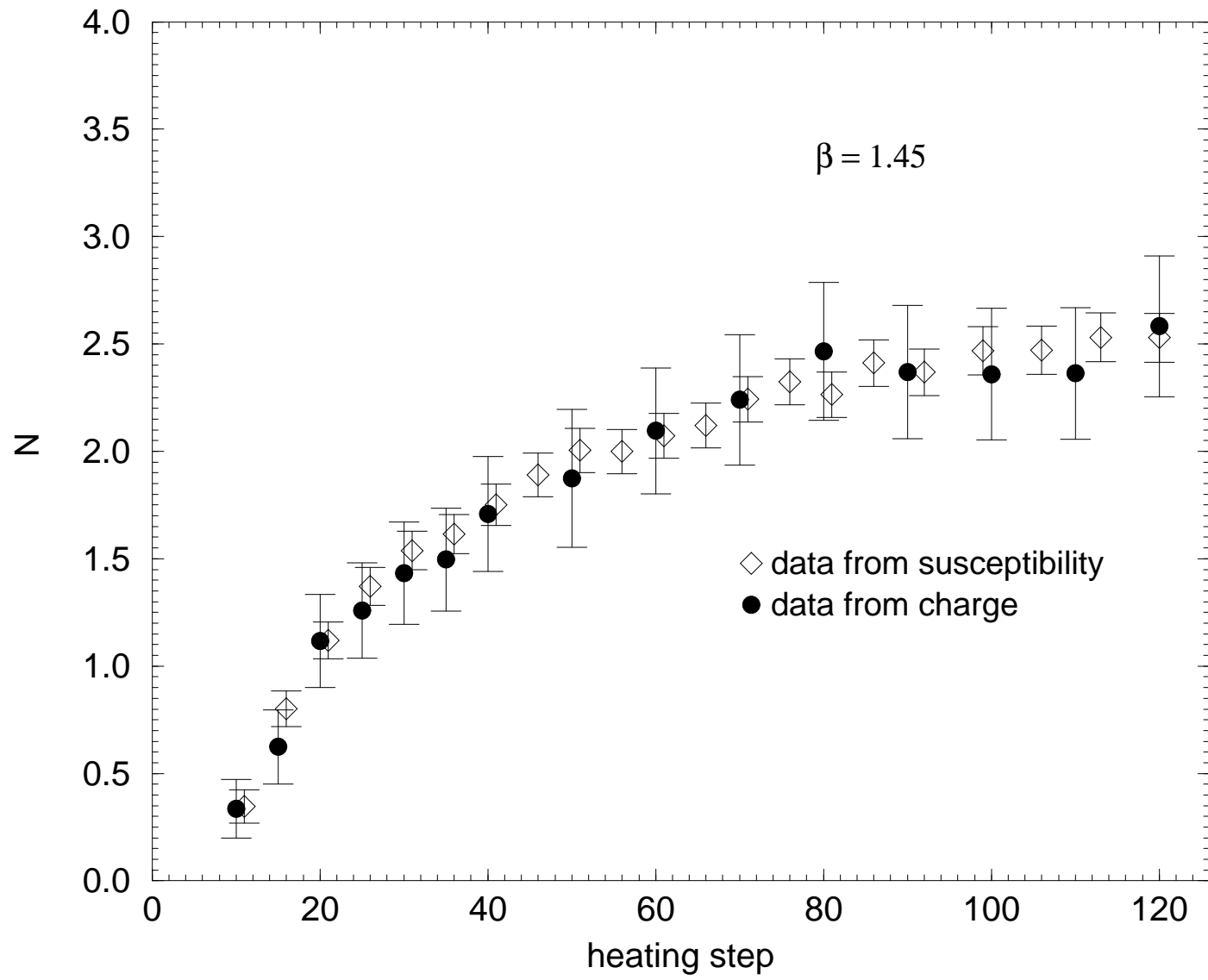


Figure 12

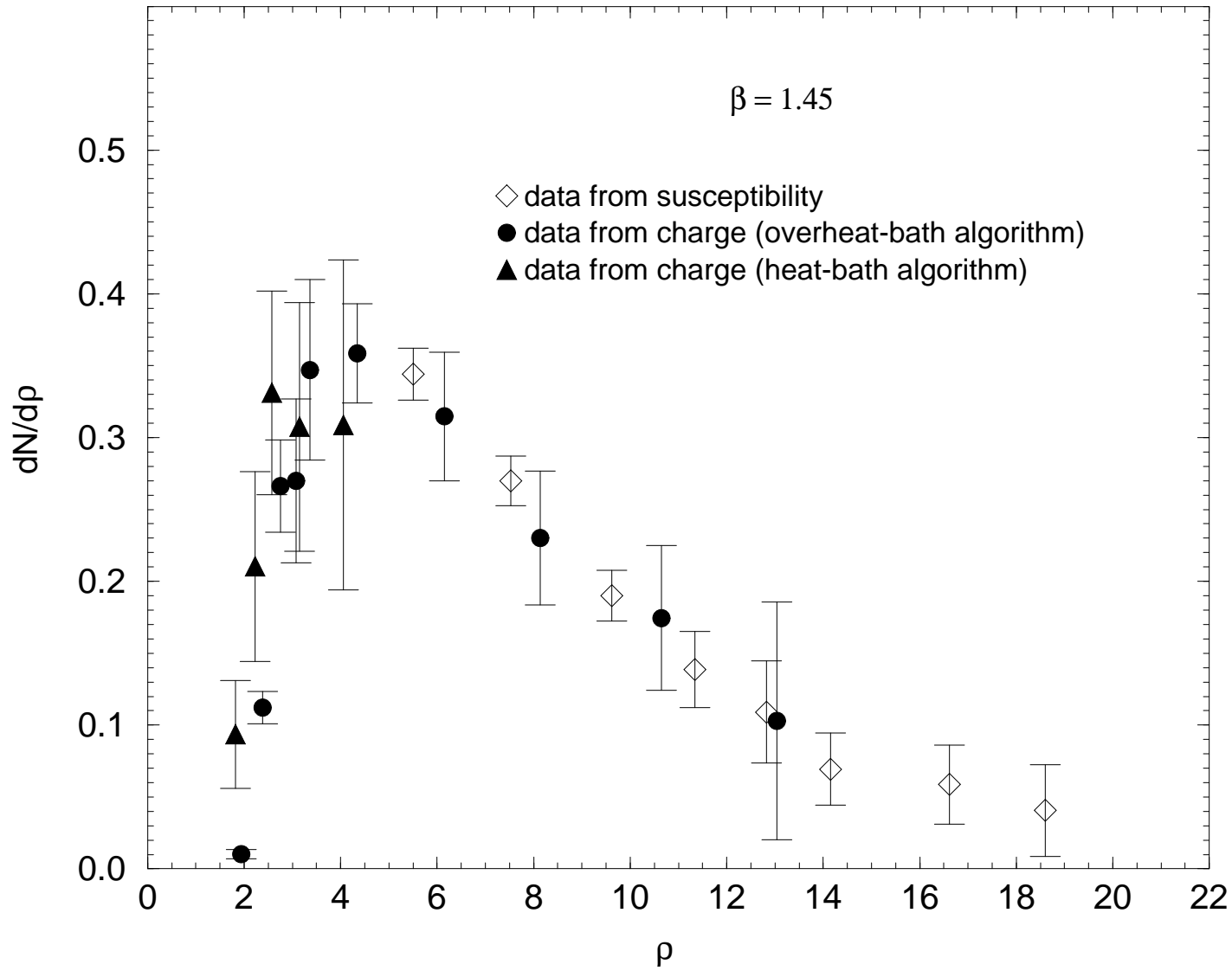


Figure 13

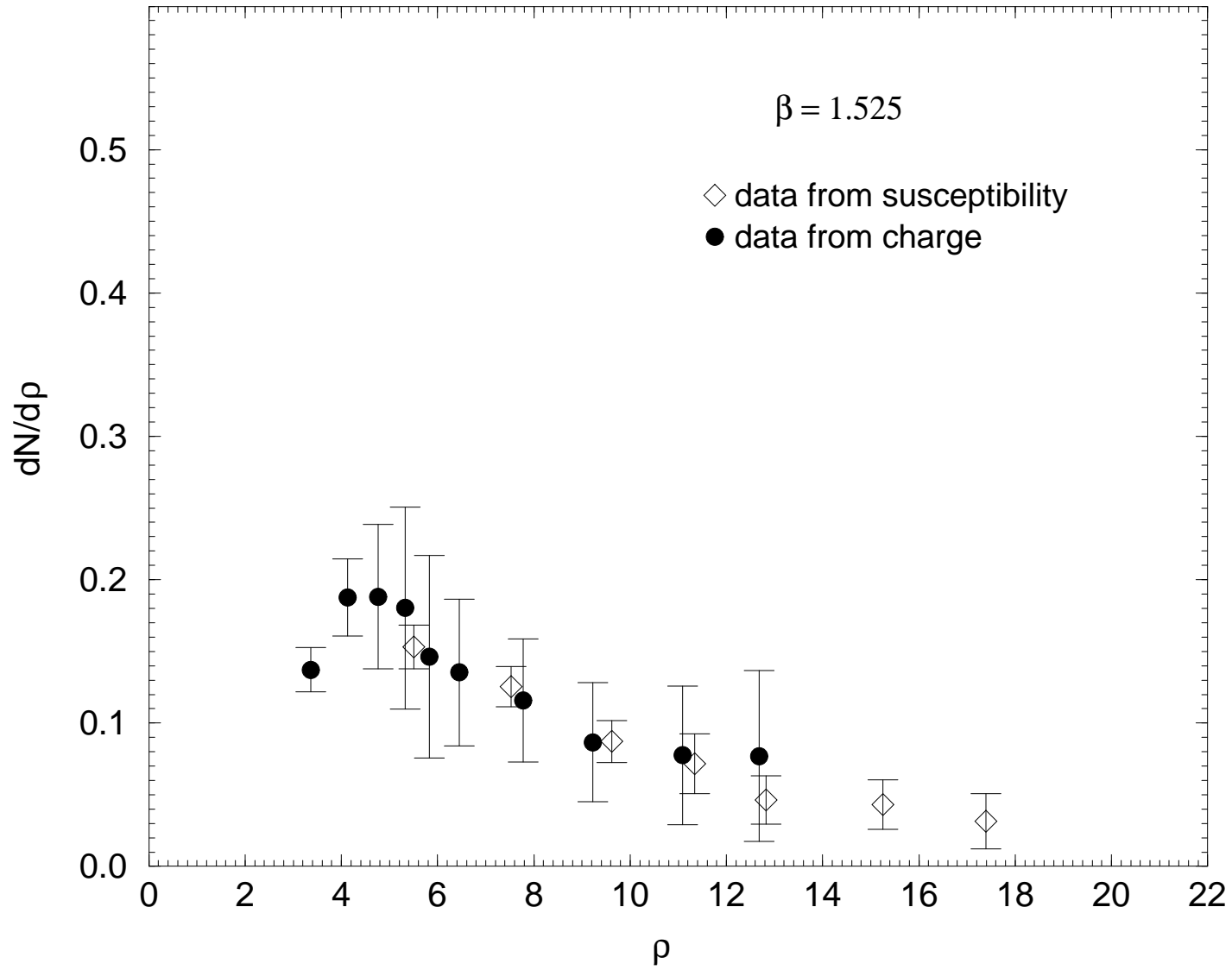


Figure 14

